Electronic Supplementary Material (ESI) for Dalton Transactions.
This journal is © The Royal Society of Chemistry 2019

Anion and Solvent Dependency of the Electronic Coupling Strength in Mixed Valent Class II Systems

Alexander Hildebrandt*, Dominique Miesel, Qing Yuan, Janine Freytag, Julia Mahrholdt and Heinrich Lang*

Technische Universität Chemnitz, Fakultät für Naturwissenschaften, Institut für Chemie, Anorganische Chemie, D-09107 Chemnitz, Germany

*Corresponding authors:

- Email: alexander.hildebrandt@chemie.tu-chemnitz.de;
Phone: +49 (0)371-531-37128; Fax: +49-(0)371-531-21219
- Email: heinrich.lang@chemie.tu-chemnitz.de;
Phone: +49 (0)371-531-21210; Fax: +49-(0)371-531-21219

Content:

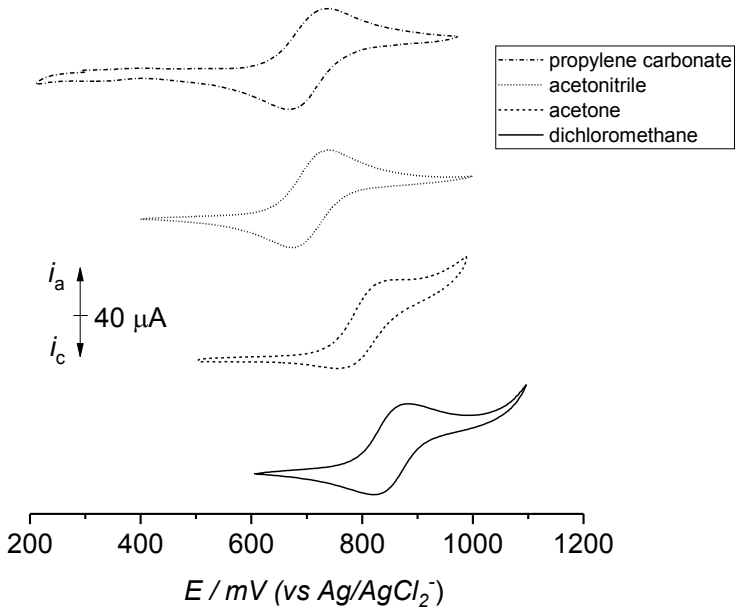

Figure SI1. Cyclic voltammograms (potential area: 200–1200 mV) of ferrocene (1.0 mmol·L^{-1}) in dichloromethane (solid), acetone (dashed), acetonitrile (dotted) and propylene carbonate (dash-dotted) at 25 °C; scan rate: 100 mV·s^{-1*}; supporting electrolyte: 0.1 mol·L^{-1} [NBu$_4$][Cl]; working electrode: glassy carbon electrode. *Please note that in order to reach reversibility of the ferrocene oxidation in the electrolyte system acetone/[NBu$_4$][Cl] scan rates of 1.5 V/s had to be used.

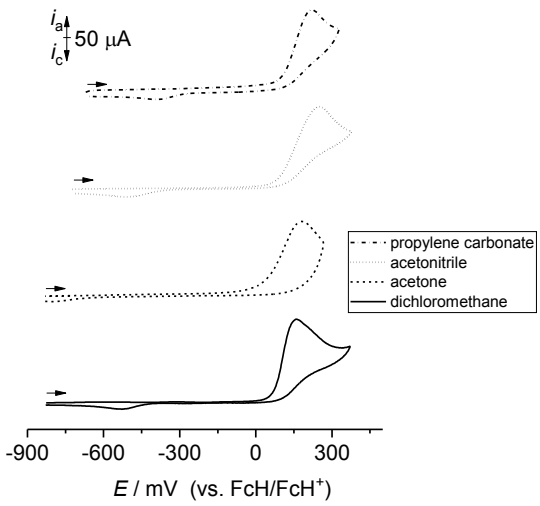

Figure SI2. Cyclic voltammograms (potential area: -900–400 mV) of **1** (1.0 mmol·L^{-1}) in dichloromethane (solid), acetone (dashed), acetonitrile (dotted) and propylene carbonate (dash-dotted) at 25 °C; scan rate: 100 mV·s^{-1}; supporting electrolyte: 0.1 mol·L^{-1} [NBu$_4$][Cl]; working electrode: glassy carbon electrode.

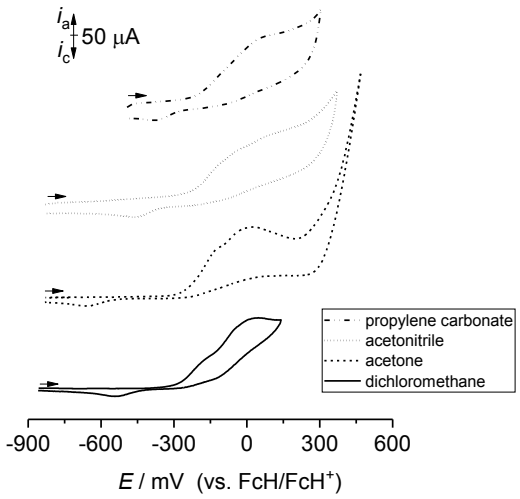

Figure SI3. Cyclic voltammograms (potential area: -900–500 mV) of **2** (1.0 mmol·L^{-1}) in dichloromethane (solid), acetone (dashed), acetonitrile (dotted) and propylene carbonate (dash-dotted) at 25 °C; scan rate: 100 mV·s^{-1}; supporting electrolyte: 0.1 mol·L^{-1} [NBu$_4$][Cl]; working electrode: glassy carbon electrode.

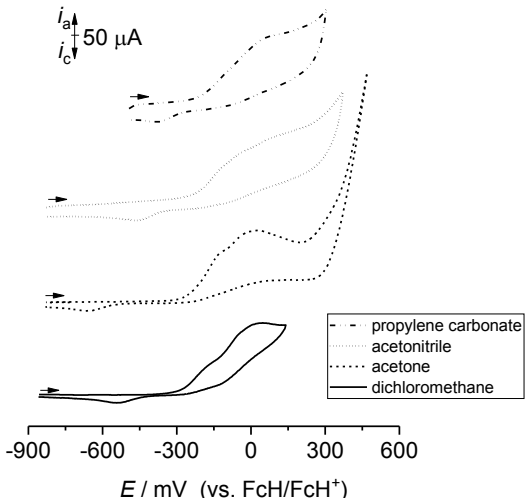

Figure SI4. Cyclic voltammograms (potential area: -900–500 mV) of **3** (1.0 mmol·L^{-1}) in dichloromethane (solid), acetone (dashed), acetonitrile (dotted) and propylene carbonate (dash-dotted) at 25 °C; scan rate: 100 mV·s^{-1}; supporting electrolyte: 0.1 mol·L^{-1} [NBu$_4$][Cl]; working electrode: glassy carbon electrode.

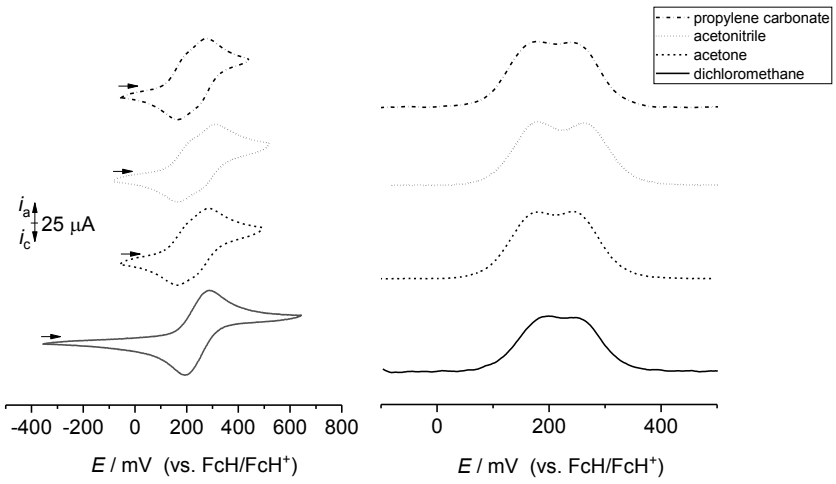

Figure SI5. Cyclic voltammograms (left; potential area: -400–700 mV; scan rate: 100 mV·s^{-1}) and square wave voltammograms (right) of **1** (1.0 mmol·L^{-1}) in dichloromethane (solid)[1], acetone (dashed), acetonitrile (dotted) and propylene carbonate (dash-dotted) at 25 °C; supporting electrolyte: 0.1 mol·L^{-1} [NBu$_4$][PF$_6$]; working electrode: glassy carbon electrode.

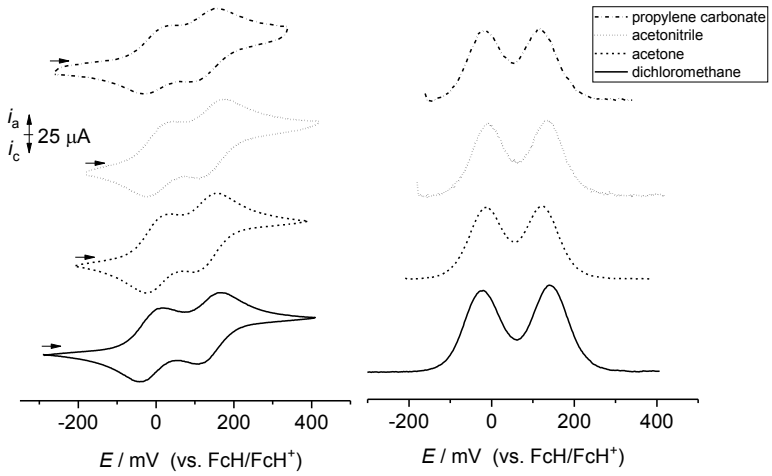

Figure SI6. Cyclic voltammograms (left; potential area: -300–400 mV; scan rate: 100 mV·s^{-1}) and square wave voltammograms (right) of **2** (1.0 mmol·L^{-1}) in dichloromethane (solid), acetone (dashed), acetonitrile (dotted) and propylene carbonate (dash-dotted) at 25 °C; supporting electrolyte: 0.1 mol·L^{-1} [NBu$_4$][PF$_6$]; working electrode: glassy carbon electrode.

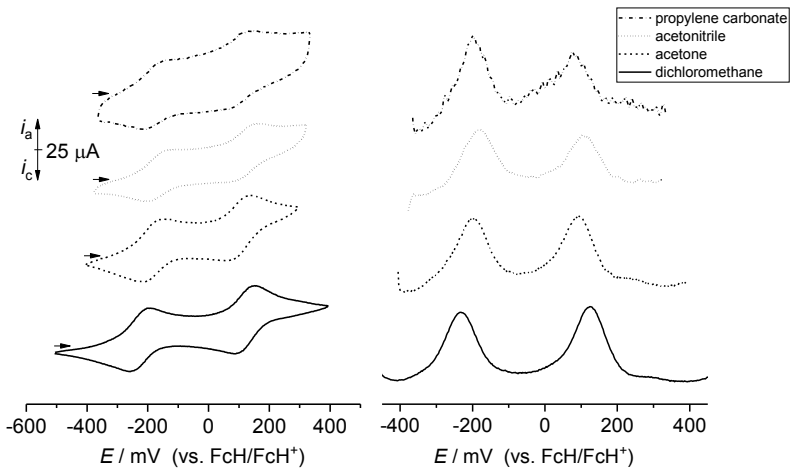

Figure SI7. Cyclic voltammograms (left; potential area: -500–400 mV; scan rate: 100 mV·s^{-1}) and square wave voltammograms (right) of **3** (1.0 mmol·L^{-1}) in dichloromethane (solid), acetone (dashed), acetonitrile (dotted) and propylene carbonate (dash-dotted) at 25 °C; supporting electrolyte: 0.1 mol·L^{-1} [NBu_4][PF_6]; working electrode: glassy carbon electrode.

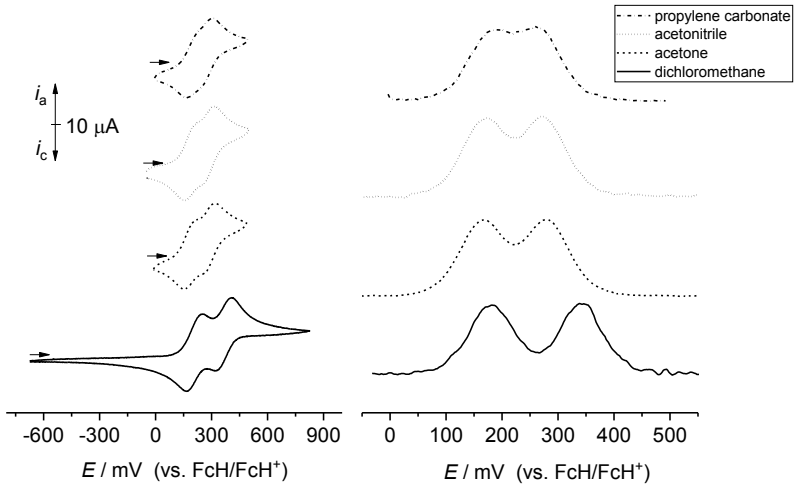

Figure SI8. Cyclic voltammograms (left; potential area: -400–700 mV; scan rate: 100 mV·s^{-1}) and square wave voltammograms (right) of **1** (1.0mmol·L^{-1}) in dichloromethane (solid)[1], acetone (dashed), acetonitrile (dotted) and propylene carbonate (dash-dotted) at 25 °C; supporting electrolyte: 0.1 mol·L^{-1} [NBu_4][BArF]; working electrode: glassy carbon electrode.

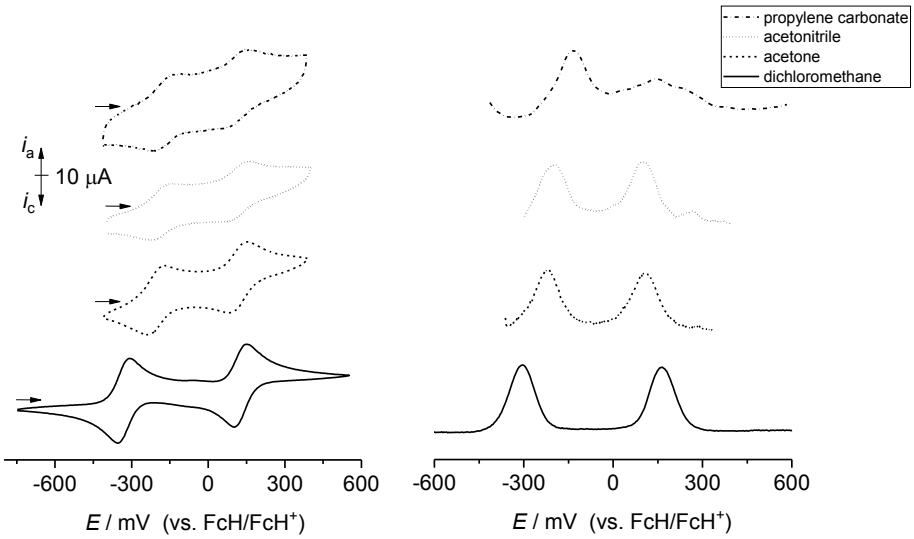

Figure SI9. Cyclic voltammograms (left; potential area: -400–700 mV; scan rate: 100 mV·s^{-1}) and square wave voltammograms (right) of **3** (1.0 mmol·L^{-1}) in dichloromethane (solid)[2], acetone (dashed), acetonitrile (dotted) and propylene carbonate (dash-dotted) at 25 °C; supporting electrolyte: 0.1 mol·L^{-1} [NBu$_4$][BArF]; working electrode: glassy carbon electrode.

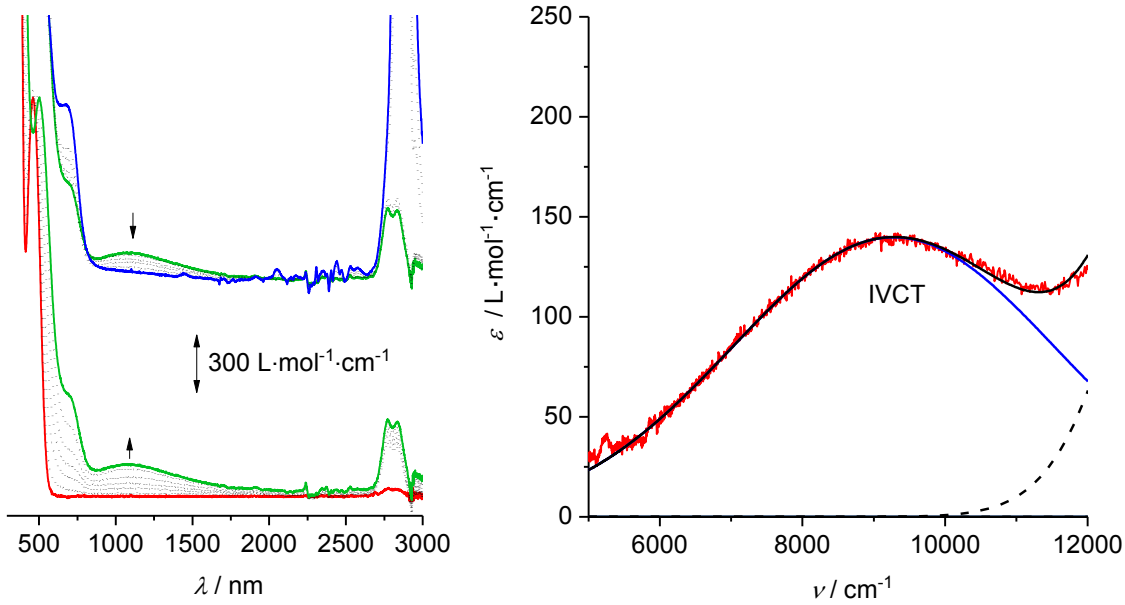

Figure SI10. Left: UV/Vis-NIR spectra of **1** at 25 °C in acetone (2.0 mmol·L^{-1}) at rising potentials (bottom: -200–700 mV; top: 700–1300 mV vs Ag/AgCl); [NBu$_4$][BArF] as supporting electrolyte (red; [**1**], green: [**1**]$^+$, blue: [**1**]$^{2+}$). Right: Deconvolution of the NIR absorptions of [**1**]$^+$ using two Gaussian shaped bands determined by spectroelectrochemistry in an OTTLE cell (red: experimental spectrum, solid black: sum of Gaussian curves, blue IVCT curve).

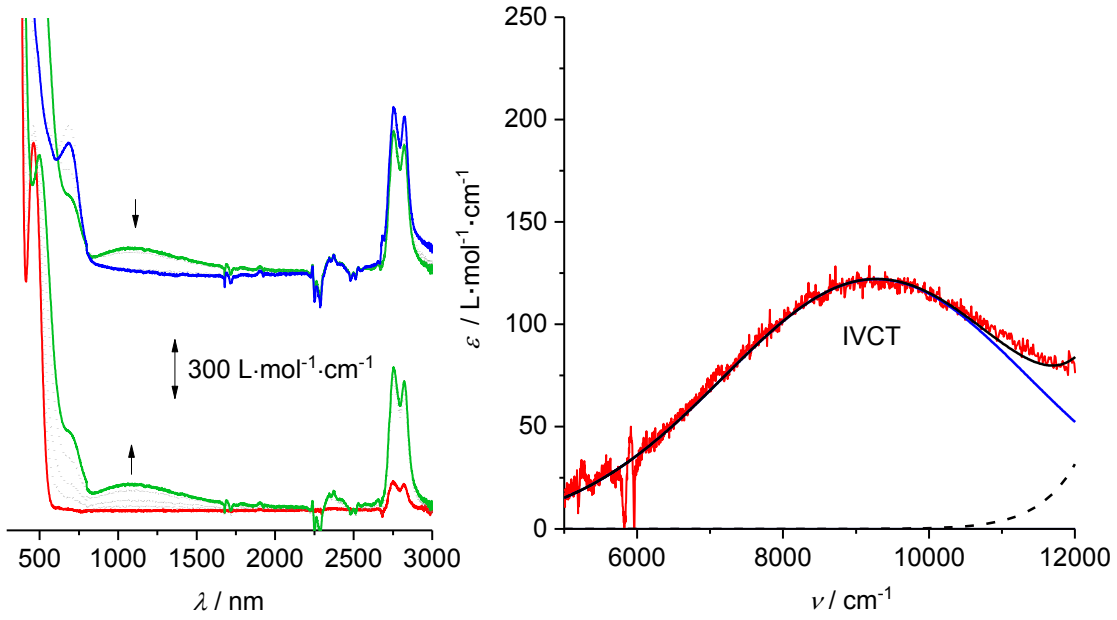

Figure SI11. Left: UV/Vis-NIR spectra of **1** at 25 °C in acetonitrile (2.0 mmol·L^{-1}) at rising potentials (bottom: -200–675 mV; top: 675–1300 mV vs Ag/AgCl); [NBu$_4$][BArF] as supporting electrolyte (red; [**1**], green: [**1**]$^{+}$, blue: [**1**]$^{2+}$). Right: Deconvolution of the NIR absorptions of [**1**]$^{+}$ using two Gaussian shaped bands determined by spectroelectrochemistry in an OTTLE cell (red: experimental spectrum, solid black: sum of Gaussian curves, blue IVCT curve).

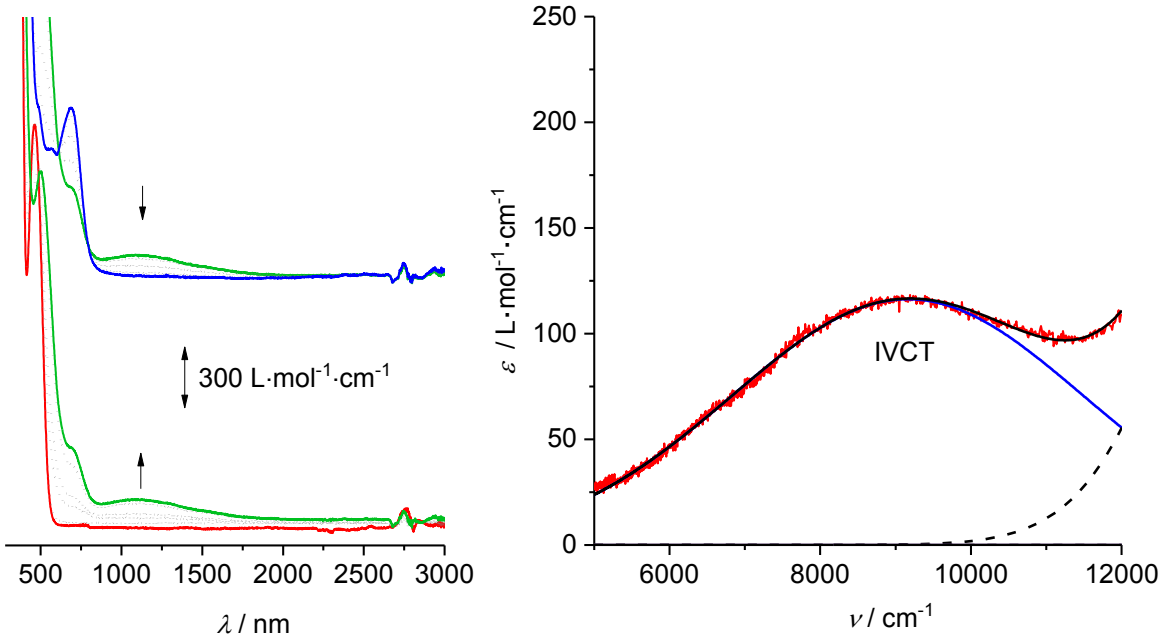

Figure SI12. Left: UV/Vis-NIR spectra of **1** at 25 °C in propylene carbonate (2.0 mmol·L^{-1}) at rising potentials (bottom: -200–600 mV; top: 600–1300 mV vs Ag/AgCl); [NBu$_4$][BArF] as supporting electrolyte (red; [**1**], green: [**1**]$^{+}$, blue: [**1**]$^{2+}$). Right: Deconvolution of the NIR absorptions of [**1**]$^{+}$ using two Gaussian shaped bands determined by spectroelectrochemistry in an OTTLE cell (red: experimental spectrum, solid black: sum of Gaussian curves, blue IVCT curve).

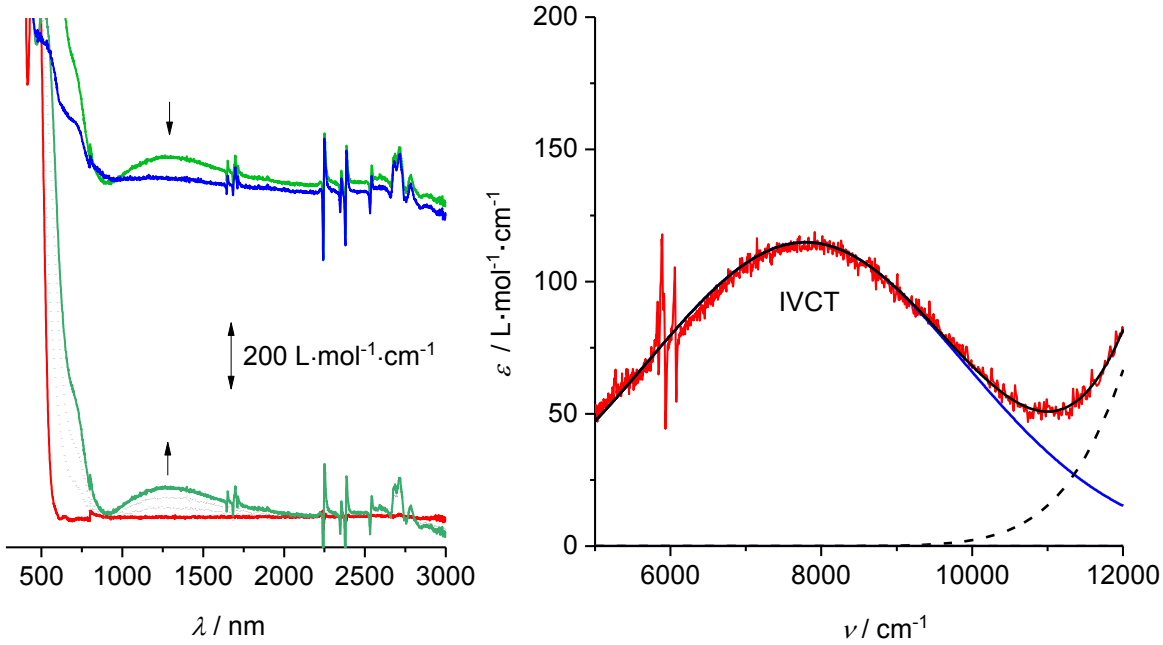

Figure SI13. Left: UV/Vis-NIR spectra of **1** at 25 °C in dichloromethane (2.0 mmol·L^{-1}) at rising potentials (bottom: -200–800 mV; top: 800–1300 mV vs Ag/AgCl); [NBu$_4$][PF$_6$] as supporting electrolyte (red; [**1**], green: [**1**]$^+$, blue: [**1**]$^{2+}$). Right: Deconvolution of the NIR absorptions of [**1**]$^+$ using two Gaussian shaped bands determined by spectroelectrochemistry in an OTTLE cell (red: experimental spectrum, solid black: sum of Gaussian curves, blue IVCT curve).

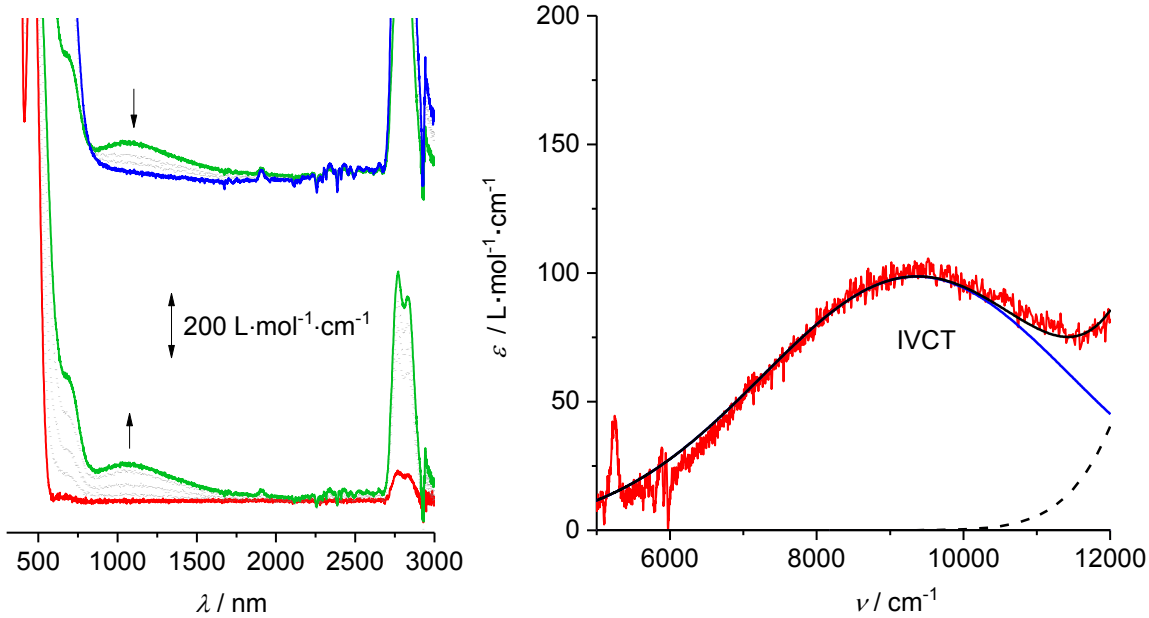

Figure SI14. Left: UV/Vis-NIR spectra of **1** at 25 °C in acetone (2.0 mmol·L^{-1}) at rising potentials (bottom: -200–650 mV; top: 650–1300 mV vs Ag/AgCl); [NBu$_4$][PF$_6$] as supporting electrolyte (red; [**1**], green: [**1**]$^+$, blue: [**1**]$^{2+}$). Right: Deconvolution of the NIR absorptions of [**1**]$^+$ using two Gaussian shaped bands determined by spectroelectrochemistry in an OTTLE cell (red: experimental spectrum, solid black: sum of Gaussian curves, blue IVCT curve).

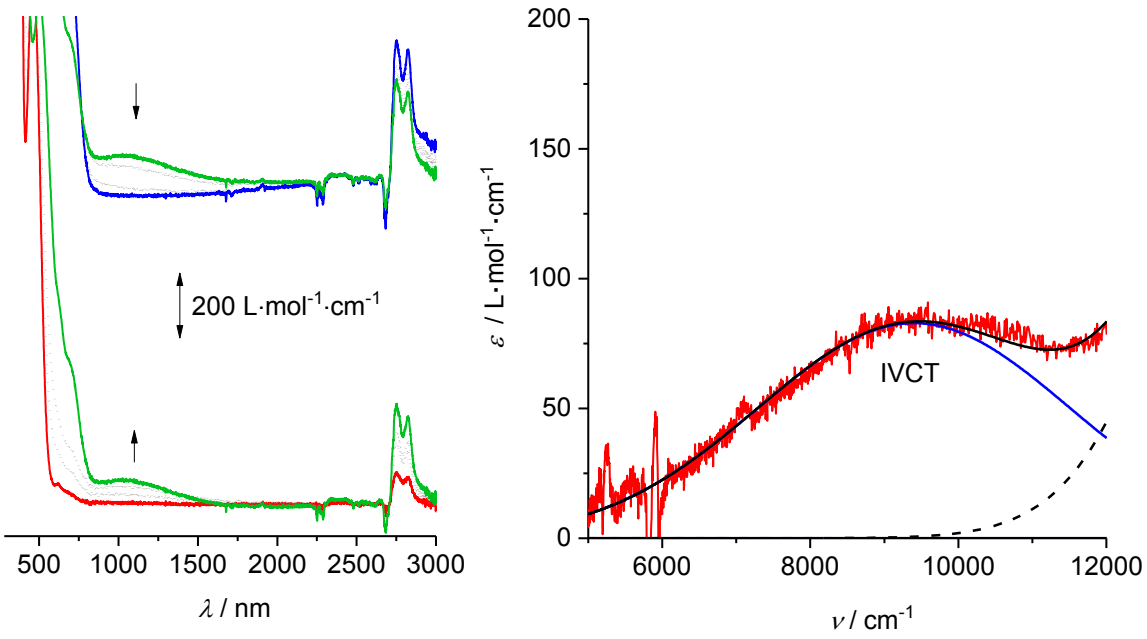

Figure SI15. Left: UV/Vis-NIR spectra of **1** at 25 °C in acetonitrile (2.0 mmol·L^{-1}) at rising potentials (bottom: -200–725 mV; top: 725–1300 mV vs Ag/AgCl); [NBu$_4$][PF$_6$] as supporting electrolyte (red; [**1**], green: [**1**]$^+$, blue: [**1**]$^{2+}$). Right: Deconvolution of the NIR absorptions of [**1**]$^+$ using two Gaussian shaped bands determined by spectroelectrochemistry in an OTTLE cell (red: experimental spectrum, solid black: sum of Gaussian curves, blue IVCT curve).

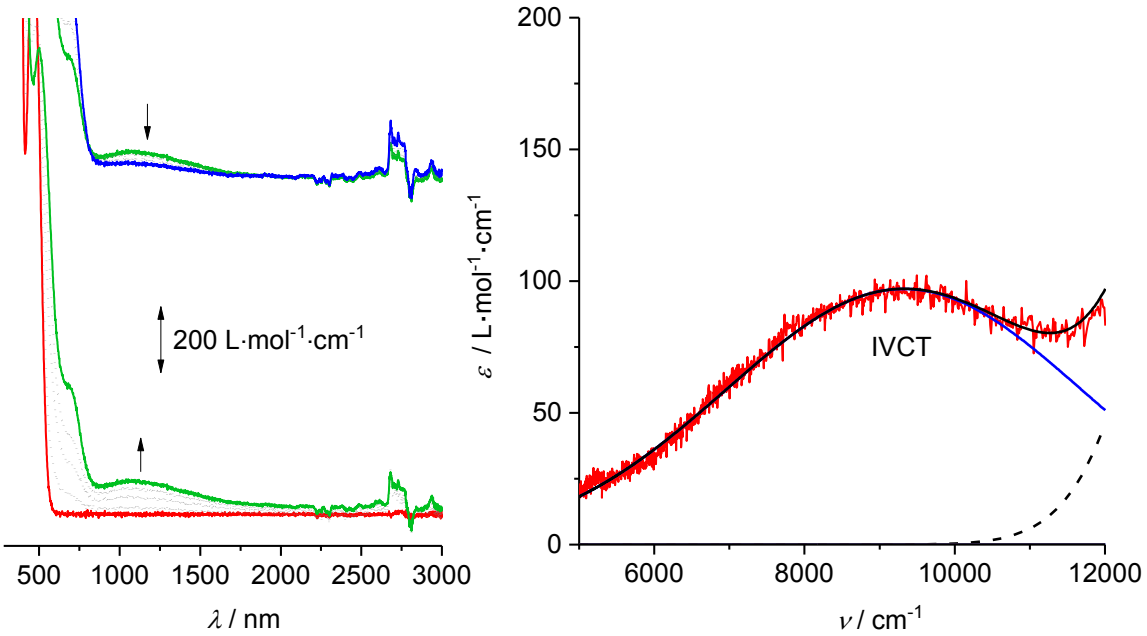

Figure SI16. Left: UV/Vis-NIR spectra of **1** at 25 °C in propylene carbonate (2.0 mmol·L^{-1}) at rising potentials (bottom: -200–875 mV; top: 875–1300 mV vs Ag/AgCl); [NBu$_4$][PF$_6$] as supporting electrolyte (red; [**1**], green: [**1**]$^+$, blue: [**1**]$^{2+}$). Right: Deconvolution of the NIR absorptions of [**1**]$^+$ using two Gaussian shaped bands determined by spectroelectrochemistry in an OTTLE cell (red: experimental spectrum, solid black: sum of Gaussian curves, blue IVCT curve).

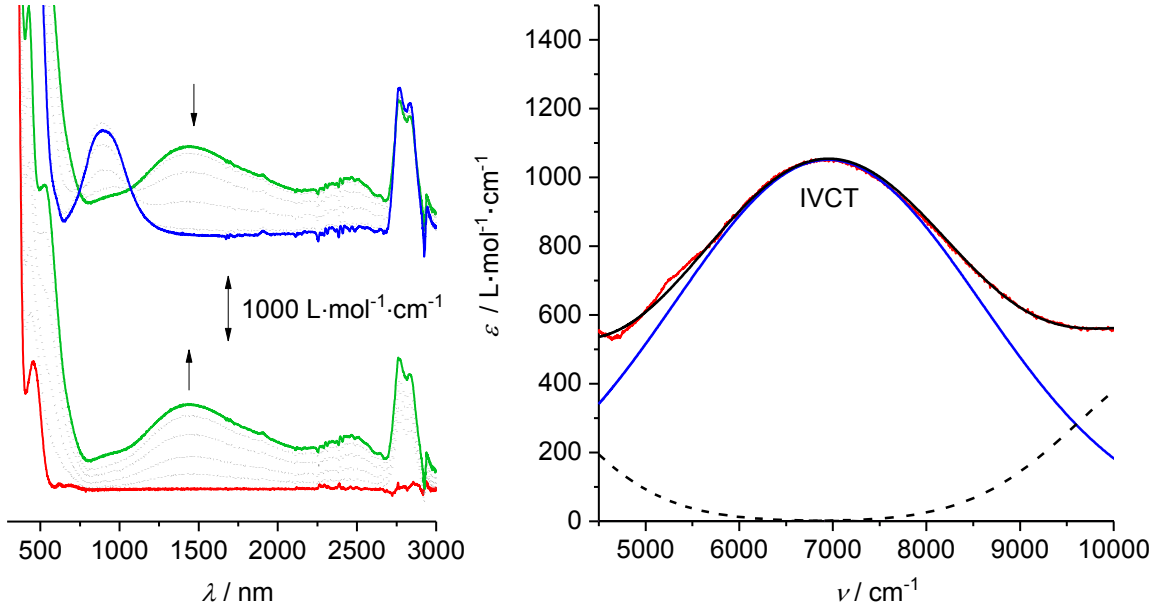

Figure SI17. Left: UV/Vis-NIR spectra of **2** at 25 °C in acetone (2.0 mmol·L^{-1}) at rising potentials (bottom: -200–525 mV; top: 525–1300 mV vs Ag/AgCl); [NBu$_4$][BArF] as supporting electrolyte (red; [**2**], green: [**2**]$^+$, blue: [**2**]$^{2+}$). Right: Deconvolution of the NIR absorptions of [**2**]$^+$ using three Gaussian shaped bands determined by spectroelectrochemistry in an OTTLE cell (red: experimental spectrum, solid black: sum of Gaussian curves, blue IVCT curve).

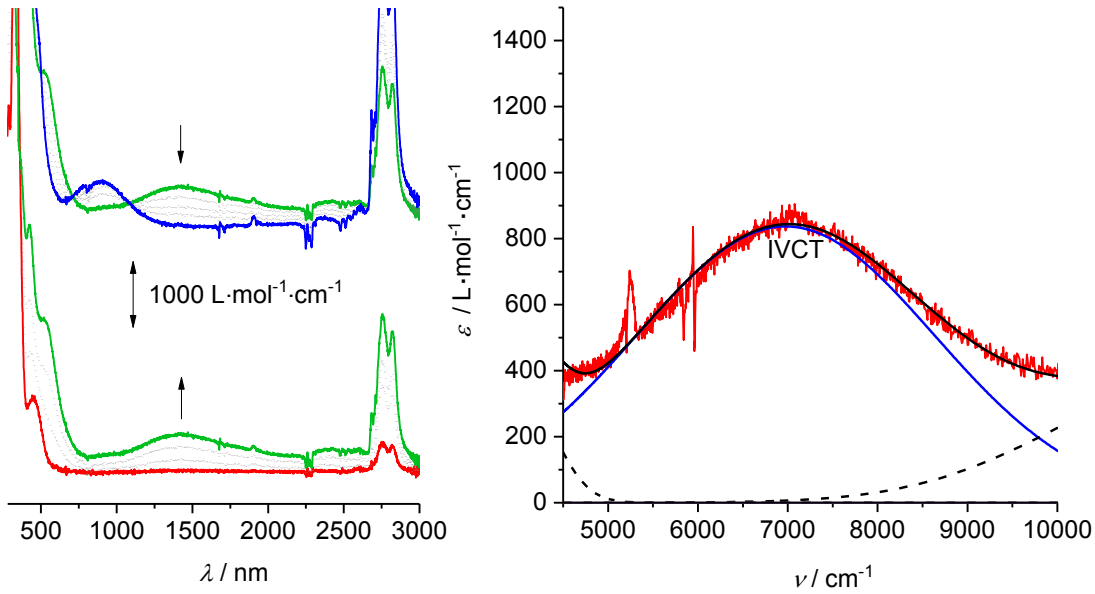

Figure SI18. Left: UV/Vis-NIR spectra of **2** at 25 °C in acetonitrile (2.0 mmol·L^{-1}) at rising potentials (bottom: -200–325 mV; top: 325–1300 mV vs Ag/AgCl); [NBu$_4$][BArF] as supporting electrolyte (red; [**2**], green: [**2**]$^+$, blue: [**2**]$^{2+}$). Right: Deconvolution of the NIR absorptions of [**2**]$^+$ using three Gaussian shaped bands determined by spectroelectrochemistry in an OTTLE cell (red: experimental spectrum, solid black: sum of Gaussian curves, blue IVCT curve).

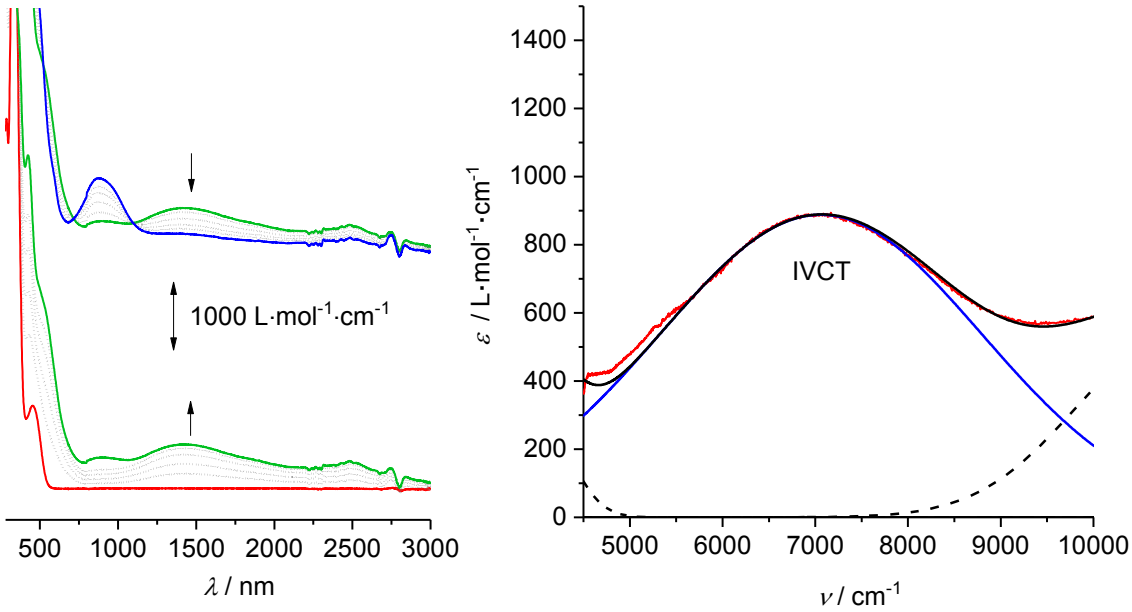

Figure SI19. Left: UV/Vis-NIR spectra of **2** at 25 °C in propylene carbonate (2.0 mmol·L^{-1}) at rising potentials (bottom: -200–575 mV; top: 575–1300 mV vs Ag/AgCl); [NBu$_4$][BArF] as supporting electrolyte (red; [**2**], green: [**2**]$^{+}$, blue: [**2**]$^{2+}$). Right: Deconvolution of the NIR absorptions of [**2**]$^{+}$ using three Gaussian shaped bands determined by spectroelectrochemistry in an OTTLE cell (red: experimental spectrum, solid black: sum of Gaussian curves, blue IVCT curve).

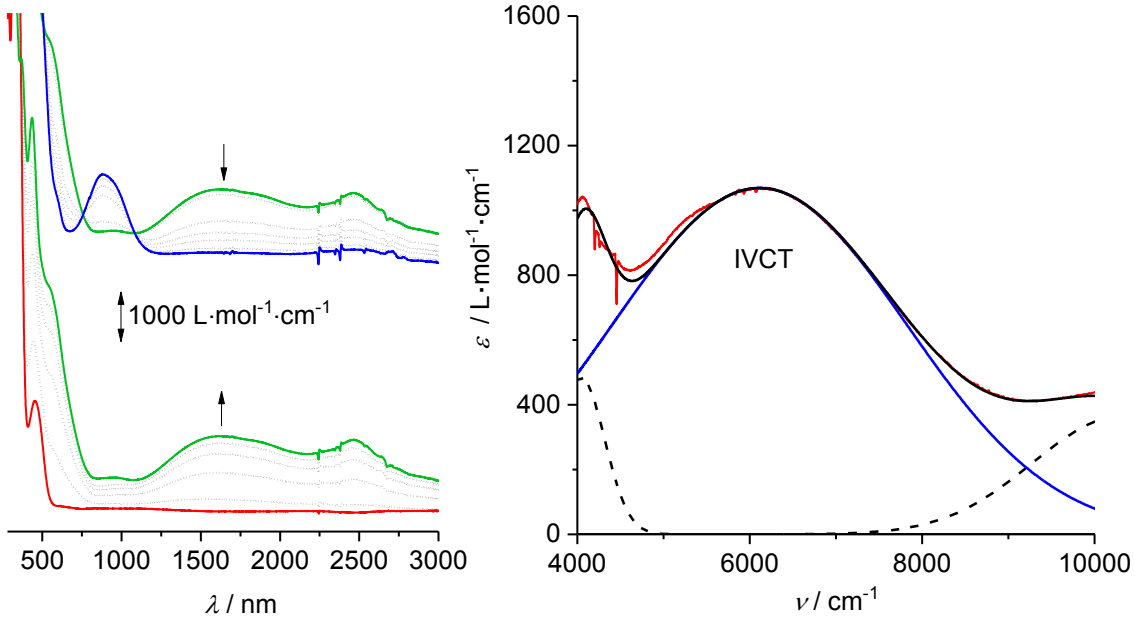

Figure SI20. Left: UV/Vis-NIR spectra of **2** at 25 °C in dichloromethane (2.0 mmol·L^{-1}) at rising potentials (bottom: -200–225 mV; top: 225–1300 mV vs Ag/AgCl); [NBu$_4$][PF$_6$] as supporting electrolyte (red; [**2**], green: [**2**]$^{+}$, blue: [**2**]$^{2+}$). Right: Deconvolution of the NIR absorptions of [**2**]$^{+}$ using three Gaussian shaped bands determined by spectroelectrochemistry in an OTTLE cell (red: experimental spectrum, solid black: sum of Gaussian curves, blue IVCT curve).

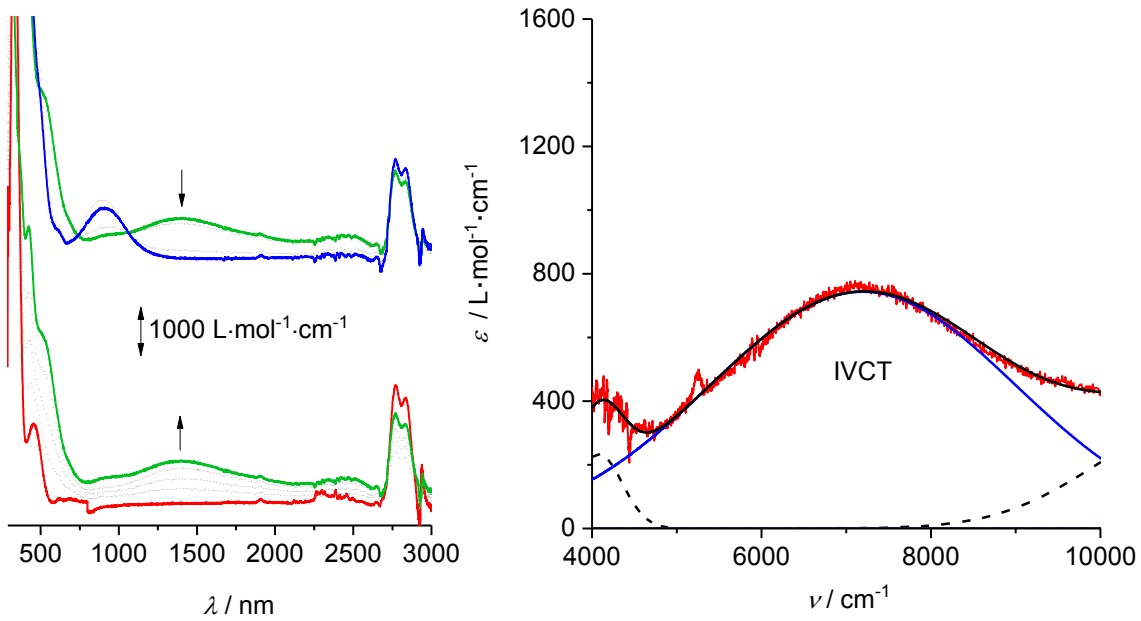

Figure SI21. Left: UV/Vis-NIR spectra of **2** at 25 °C in acetone (2.0 mmol·L^{-1}) at rising potentials (bottom: -200–700 mV; top: 700–1300 mV vs Ag/AgCl); [NBu$_4$][PF$_6$] as supporting electrolyte (red; [**2**], green: [**2**]$^{+}$, blue: [**2**]$^{2+}$). Right: Deconvolution of the NIR absorptions of [**2**]$^{+}$ using three Gaussian shaped bands determined by spectroelectrochemistry in an OTTLE cell (red: experimental spectrum, solid black: sum of Gaussian curves, blue IVCT curve).

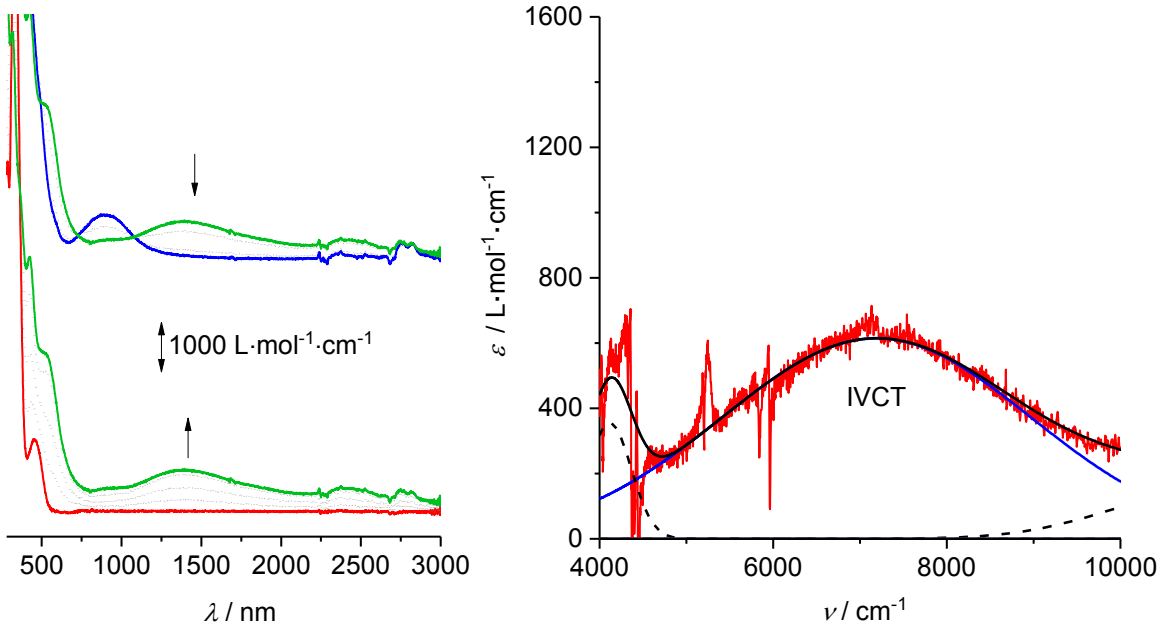

Figure SI22. Left: UV/Vis-NIR spectra of **2** at 25 °C in acetonitrile (2.0 mmol·L^{-1}) at rising potentials (bottom: -200–475 mV; top: 475–1300 mV vs Ag/AgCl); [NBu$_4$][PF$_6$] as supporting electrolyte (red; [**2**], green: [**2**]$^{+}$, blue: [**2**]$^{2+}$). Right: Deconvolution of the NIR absorptions of [**2**]$^{+}$ using three Gaussian shaped bands determined by spectroelectrochemistry in an OTTLE cell (red: experimental spectrum, solid black: sum of Gaussian curves, blue IVCT curve).

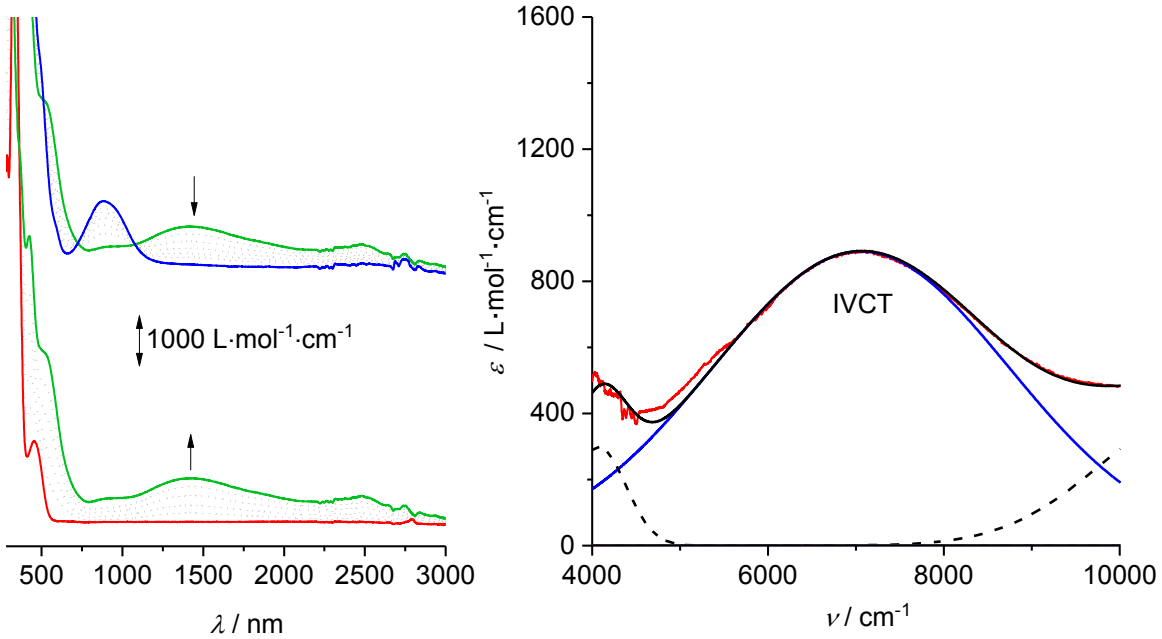

Figure SI23. Left: UV/Vis-NIR spectra of **2** at 25 °C in propylene carbonate (2.0 mmol·L^{-1}) at rising potentials (bottom: -200–650 mV; top: 650–1300 mV vs Ag/AgCl); [NBu$_4$][PF$_6$] as supporting electrolyte (red; [**2**], green: [**2**]$^{+}$, blue: [**2**]$^{2+}$). Right: Deconvolution of the NIR absorptions of [**2**]$^{+}$ using three Gaussian shaped bands determined by spectroelectrochemistry in an OTTLE cell (red: experimental spectrum, solid black: sum of Gaussian curves, blue IVCT curve).

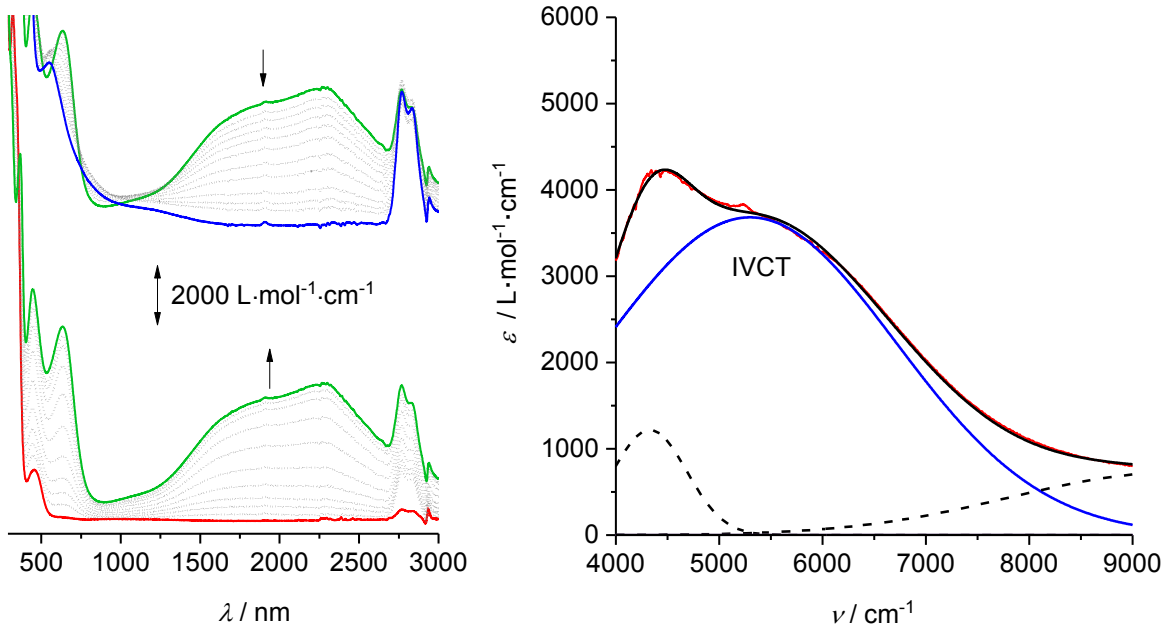

Figure SI24. Left: UV/Vis-NIR spectra of **3** at 25 °C in acetone (1.0 mmol·L^{-1}) at rising potentials (bottom: -200–400 mV; top: 400–1300 mV vs Ag/AgCl); [NBu$_4$][BArF] as supporting electrolyte (red; [**3**], green: [**3**]$^{+}$, blue: [**3**]$^{2+}$). Right: Deconvolution of the NIR absorptions of [**3**]$^{+}$ using three Gaussian shaped bands determined by spectroelectrochemistry in an OTTLE cell (red: experimental spectrum, solid black: sum of Gaussian curves, blue IVCT curve).

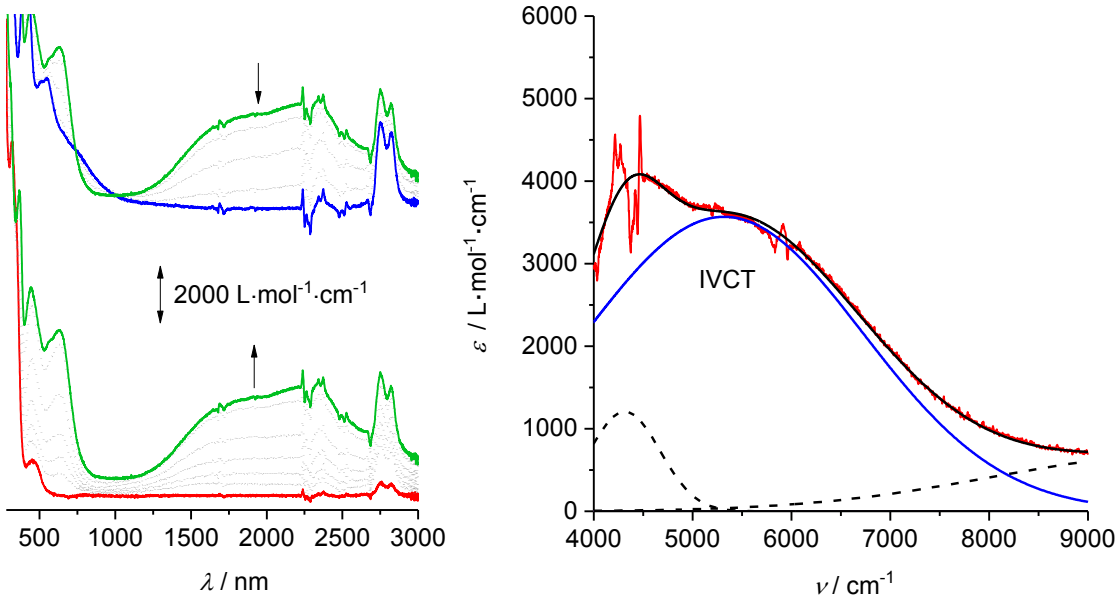

Figure SI25. Left: UV/Vis-NIR spectra of **3** at 25 °C in acetonitrile (1.0 mmol·L^{-1}) at rising potentials (bottom: -200–225 mV; top: 225–1300 mV vs Ag/AgCl); [NBu$_4$][BArF] as supporting electrolyte (red; [**3**], green: [**3**]$^{+}$, blue: [**3**]$^{2+}$). Right: Deconvolution of the NIR absorptions of [**3**]$^{+}$ using three Gaussian shaped bands determined by spectroelectrochemistry in an OTTLE cell (red: experimental spectrum, solid black: sum of Gaussian curves, blue IVCT curve).

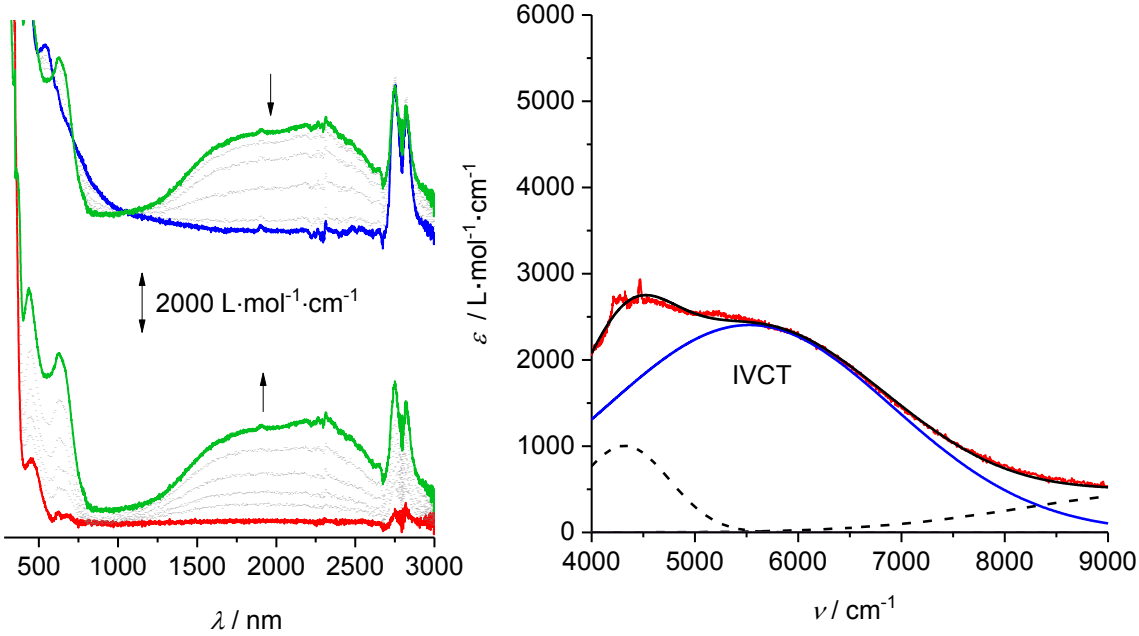

Figure SI26. Left: UV/Vis-NIR spectra of **3** at 25 °C in propylene carbonate (1.0 mmol·L^{-1}) at rising potentials (bottom: -200–400 mV; top: 400–1300 mV vs Ag/AgCl); [NBu$_4$][BArF] as supporting electrolyte (red; [**3**], green: [**3**]$^{+}$, blue: [**3**]$^{2+}$). Right: Deconvolution of the NIR absorptions of [**3**]$^{+}$ using three Gaussian shaped bands determined by spectroelectrochemistry in an OTTLE cell (red: experimental spectrum, solid black: sum of Gaussian curves, blue IVCT curve).

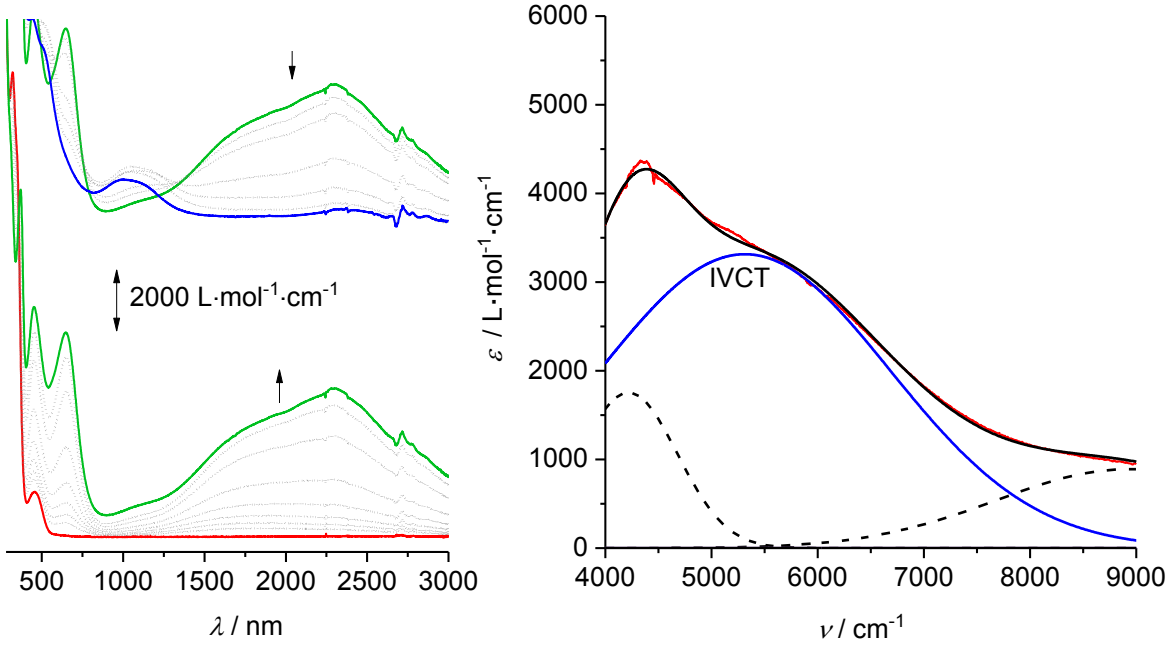

Figure SI27. Left: UV/Vis-NIR spectra of **3** at 25 °C in dichloromethane (1.0 mmol·L^{-1}) at rising potentials (bottom: -200–275 mV; top: 275–1300 mV vs Ag/AgCl); $[NBu_4][PF_6]$ as supporting electrolyte (red; [**3**], green: [**3**]$^{+}$, blue: [**3**]$^{2+}$). Right: Deconvolution of the NIR absorptions of [**3**]$^{+}$ using three Gaussian shaped bands determined by spectroelectrochemistry in an OTTLE cell (red: experimental spectrum, solid black: sum of Gaussian curves, blue IVCT curve).

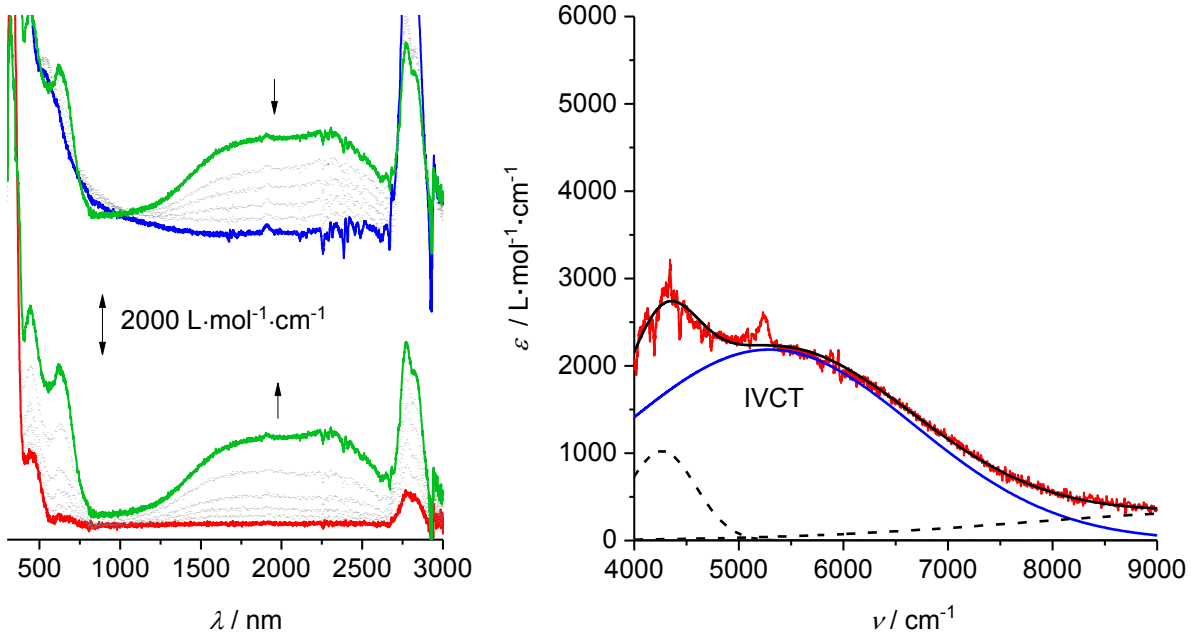

Figure SI28. Left: UV/Vis-NIR spectra of **3** at 25 °C in acetone (1.0 mmol·L^{-1}) at rising potentials (bottom: -200–350 mV; top: 350–1300 mV vs Ag/AgCl); $[NBu_4][PF_6]$ as supporting electrolyte (red; [**3**], green: [**3**]$^{+}$, blue: [**3**]$^{2+}$). Right: Deconvolution of the NIR absorptions of [**3**]$^{+}$ using three Gaussian shaped bands determined by spectroelectrochemistry in an OTTLE cell (red: experimental spectrum, solid black: sum of Gaussian curves, blue IVCT curve).

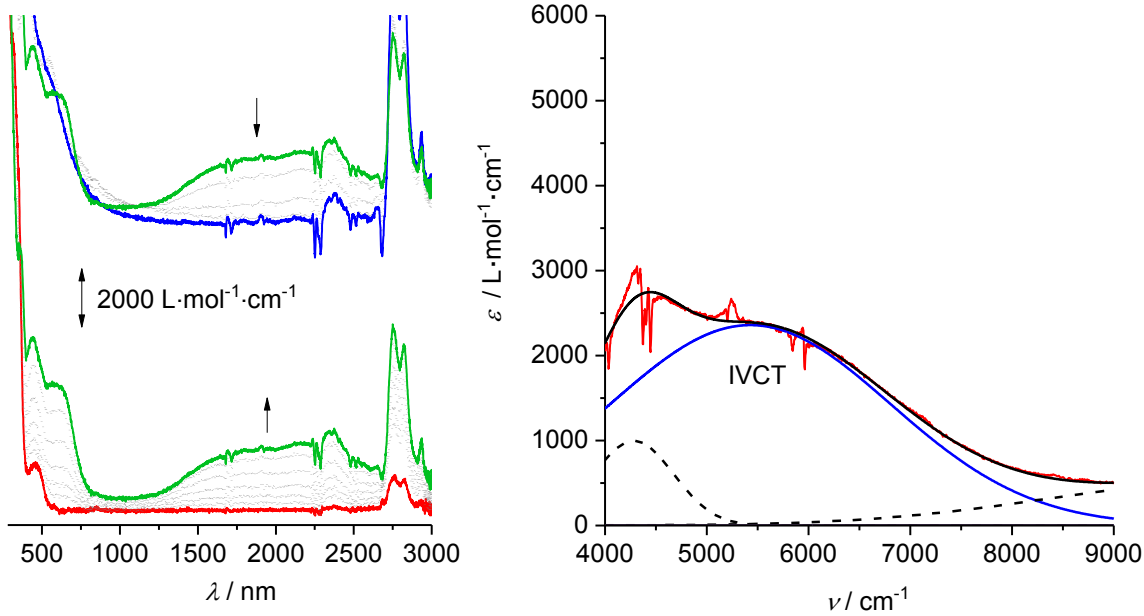

Figure SI29. Left: UV/Vis-NIR spectra of **3** at 25 °C in acetonitrile (1.0 mmol·L^{-1}) at rising potentials (bottom: -200–275 mV; top: 275–1300 mV vs Ag/AgCl); [NBu$_4$][PF$_6$] as supporting electrolyte (red; [**3**], green: [**3**]$^{+}$, blue: [**3**]$^{2+}$). Right: Deconvolution of the NIR absorptions of [**3**]$^{+}$ using three Gaussian shaped bands determined by spectroelectrochemistry in an OTTLE cell (red: experimental spectrum, solid black: sum of Gaussian curves, blue IVCT curve).

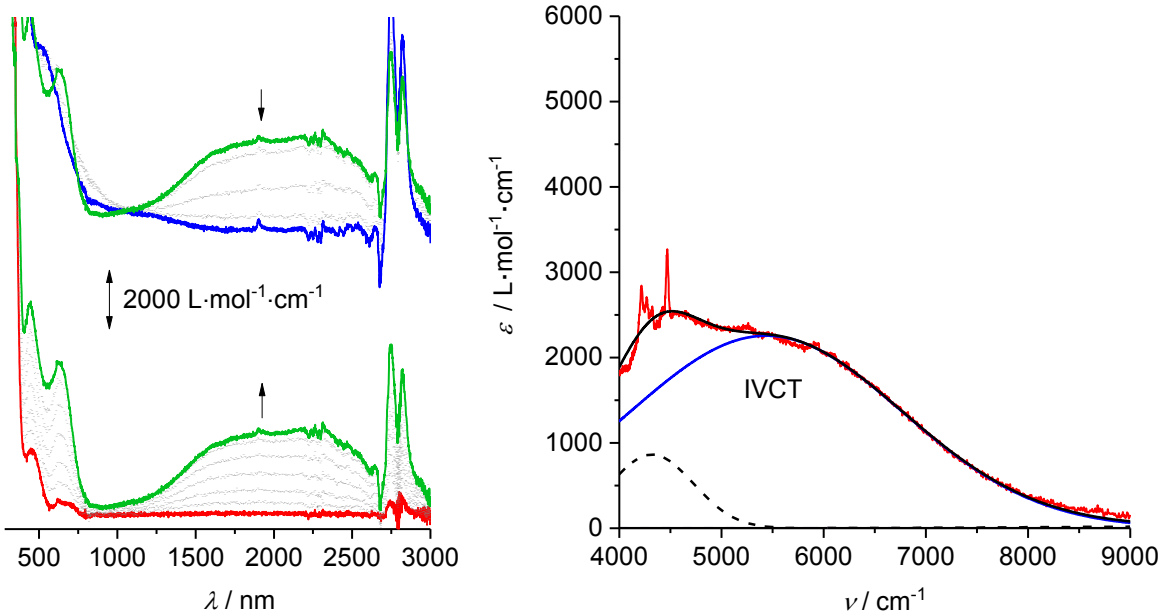

Figure SI30. Left: UV/Vis-NIR spectra of **3** at 25 °C in propylene carbonate (1.0 mmol·L^{-1}) at rising potentials (bottom: -200–450 mV; top: 450–1300 mV vs Ag/AgCl); [NBu$_4$][PF$_6$] as supporting electrolyte (red; [**3**], green: [**3**]$^{+}$, blue: [**3**]$^{2+}$). Right: Deconvolution of the NIR absorptions of [**3**]$^{+}$ using three Gaussian shaped bands determined by spectroelectrochemistry in an OTTLE cell (red: experimental spectrum, solid black: sum of Gaussian curves, blue IVCT curve).

References

1 (a) A. Hildebrandt, D. Schaarschmidt, L. van As, J. C. Swarts and H. Lang, *Inorg. Chim. Acta*, 2011, **374**, 112.

(b) A. Hildebrandt and H. Lang, *Organometallics*, 2013, **32**, 2993.

2 A. Hildebrandt and H. Lang, *Dalton Trans.*, 2011, **40**, 11831.